EurJOC European Journal of Organic Chemistry

FULL PAPER

DOI: 10.1002/ejoc.201300487

Synthesis, Structural, and Photophysical Properties of the First Member of the Class of Pyrene-Based [4]Helicenes

Jian-Yong Hu,[a,b] Xing Feng,[a] Arjun Paudel,[a] Hirotsugu Tomiyasu,[a] Ummey Rayhan,[a] Pierre Thuéry,[c] Mark R. J. Elsegood,[d] Carl Redshaw,[e] and Takehiko Yamato*[a]

Keywords: Fused-ring systems / Wittig reactions / Cyclization / Helical structures / Optoelectronic properties

A convenient route to a new class of pyrene-based [4]helicenes is presented. Wittig reaction of 7-*tert*-butyl-1,3-dimethyl-5-formylpyrene with benzyltriphenylphosphonium salts in the presence of *n*BuLi afforded 7-*tert*-butyl-1,3-dimethyl-5-(phenylethenyl)pyrenes, from which 4,5-naphthalene annulated aromatic [4]helicenes, namely 7-*tert*-butyl-1,3-dimethyl-13-methoxydibenzo[*ij*,*no*]tetraphene and 7-*tert*-butyl-1,3,12,14-tetramethyldibenzo[*ij*,*no*]tetraphene, were obtained by photoinduced intramolecular cyclization. The chemical structures of these [4]helicenes were determined on the basis of their elemental analyses and spectroscopic data. The helicity in the synthesized [4]helicene induced by the presence of the second methyl group in the fjord region is discussed in detail. The photophysical and electrochemical properties of these newly developed [4]helicenes were fully investigated by UV/Vis absorption and photoluminescence spectrphotometry, and cyclic voltammetry (CV), and the crystal structures were determined for two examples.

Introduction

Although described in the early 20th century literature by Weitzenbock and co-workers, as well as by Mayer and Oppenheimer,[1] the isolation of the first tetrahelicene (**I**; Figure 1) was not confirmed until the early 1930s when Cook and Heweit reinvestigated their work.[2,3] Parent benzo[*c*]phenanthrene (B[C]Ph, **I**) is the smallest polycyclic aromatic hydrocarbon (PAH) with a fjord region. As the first member of the [*n*]helicene family,[4] it has a twisted framework with an angle of 27° between the A and D rings, as shown by the X-ray structure.[5] Focusing on structure–activity relationships, the 3-, 4-, 5-, and 6-methylated derivatives of such compounds were found to be tumorigenic in mouse skin, but the 1- and 2-methyl derivatives were reported to be less active than the parent (B[C]Ph).[6] Fluorine substitution on the benzo ring was found to exhibit enhanced tumorigenicity relative to parent **I**, except for the 2-fluoro derivative, which was less active.[7] In addition, nitration, acetylation, and bromination of the parent **I** were investigated by Newman in the 1940s; his studies showed preferential substitution at C-5.[8]

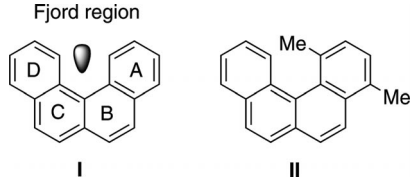

Figure 1. Structures of tetrahelicenes **I** and **II**.

The influence of planarity on the metabolic activation and DNA-binding properties of PAHs were studied by Lakshman et al. in 2000,[9] who reported that the increased nonplanarity in this type of PAH lowered their ability to be metabolically activated to form DNA-damaging adducts. Interestingly, this report also described a convenient synthetic route to 1,4-dimethylB[C]Ph (**II**), its (±)-*trans*-9,10-dihyrodiol, as well as the (±)-9β,10α,1α-epoxide. Comparative metabolic activation and DNA-binding of B[C]Ph, 1,4-DMB[C]Ph, and their dihydrodiols have been investigated by using mammary carcinoma MCF-7 cells. This study also showed that a methyl group in the fjord region can induce helicity in these small hydrocarbons, resulting in atropisomerism (*P* and *M* helicity). Methyl substitution in the highly congested fjord region increased skeletal distortion from 27° for the A/D ring angle in B[C]Ph (**I**) to 30° for that in 1,4-DMB[C]Ph (**II**).[10]

[a] Department of Applied Chemistry, Faculty of Science and Engineering, Saga University,
Honjo-machi 1, Saga-shi, Saga 840-8502, Japan
E-mail: yamatot@cc.saga-u.ac.jp
Homepage: http://www.fusion.saga-u.ac.jp
[b] Emergent Molecular Function Research Group, RIKEN Center for Emergent Matter Science (CEMS),
Wako, Saitama 351-0198, Japan
[c] Service de Chimie Moléculaire, DSM, DRECAM, CNRS URA 331, CEA Saclay,
91191 Gif-sur-Yvette, France
[d] Chemistry Department, Loughborough University,
Loughborough, LE11 3TU, UK
[e] Department of Chemistry, The University of Hull,
Hull, HU6 7RX, UK

Supporting information for this article is available on the WWW under http://dx.doi.org/10.1002/ejoc.201300487.

Photochemical ring closure of appropriate stilbenes to phenanthrenes has proven to be a useful method for the synthesis of several angular-fused PAHs,[11] and as an extension of this method, the synthesis of fjord-region dihydrodiols has been documented.[12] However, for this study, the suitability of this method was not known because the introduction in the fjord region of at least one methyl group in the course of pyrene-based photocyclization had not then been documented.

Electrophilic substitution of pyrene only occurs at the 1-, 3-, 6-, and 8-positions, and not at the other positions (2, 4, 5, 7, 9, and 10).[13,14] Therefore pyrenes substituted at the latter positions must be prepared in ways other than by direct electrophilic substitution of pyrene itself. Regioselective electrophilic substitution at the 5- or 5,9-positions is still challenging. We previously reported the convenient preparative synthesis of 7-*tert*-butyl-1,3-dimethylpyrene from pyrene in five steps, which involved the formylation of 7-*tert*-butyl-1,3-dimethylpyrene and Wolff–Kishner reduction.[15,16] This compound is a convenient starting material for the preparation of 5- and 5,9-disubstituted 1,3-dimethylpyrenes by electrophilic substitution because the active 6- and 8-positions of the pyrene ring are protected by the *tert*-butyl group.

In this work, the electrophilic aromatic substitution of 7-*tert*-butyl-1,3-dimethylpyrene selectively afforded 5-monoformyl substitution product depending on the Lewis acid catalysts that were used for the preparation of the first members of a new class of pyrene-based [4]helicenes. These contain at least one methyl group in the fjord region. Their photophysical and electrochemical properties will be presented in full.

Results and Discussion

Synthesis

7-*tert*-Butyl-1,3-dimethylpyrene (**1**) was prepared according to the previously reported procedure.[15,16] Pyrene **1** was then formylated with dichloromethyl methyl ether under various conditions. Under the optimum conditions, the reaction took place at room temperature for 3 h in the presence of titanium tetrachloride selectively at the 5-position to give the corresponding 5-monoformylated product **2** in 69% yield (Scheme 1).

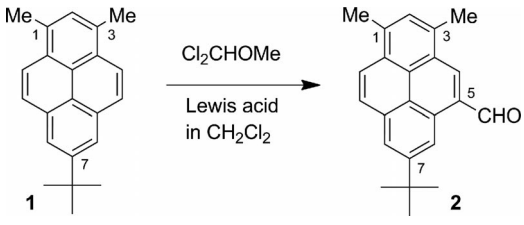

Scheme 1. Formylation of 7-*tert*-butyl-1,3-dimethylpyrene (**1**).

The structure of **2** was assigned by spectroscopic data and elemental analysis. The ^{1}H NMR spectrum (300 MHz, $CDCl_3$) of **2** shows a set of doublets with a *meta* coupling constant (J = 1.8 Hz) at δ = 8.25 (8-H) and 9.73 (6-H) ppm, as well as two singlets at δ = 7.69 (2-H) and 8.61 (4-H) ppm. Similarly, a set of doublets with an *ortho* coupling constant (J = 9.2 Hz) at δ = 8.02 and 8.12 ppm were assigned to the protons at the 9- and 10-positions on the pyrene ring, respectively. The singlet peak at δ = 10.49 ppm was assigned to the formyl proton. These data strongly support a structure of 7-*tert*-butyl-1,3-dimethylpyrene-5-carbaldehyde (**2**), and strongly suggest that the *tert*-butyl group on the pyrene ring protects the pyrene from electrophilic attack at the 6,8-positions, as well as the methyl groups at the 1,3-positions inhibiting electrophilic attack at the 4,10-positions.

The reaction of **2** and (4-methoxybenzyl)triphenylphosphonium chloride (**3**) with *n*-butyllithium in THF gave the desired 7-*tert*-butyl-1,3-dimethyl-5-(4-methoxyphenylethenyl)pyrene [(*E*)-**4**; Scheme 2]. Only the *E* isomer was isolated in 72% yield by silica gel column chromatography and recrystallization from hexane and dichloromethane. The structure of (*E*)-**4** was determined by elemental analysis and spectroscopic data. In ^{1}H NMR spectroscopy, a singlet from the olefinic protons of the *E* isomer should be observed at a lower field ($\delta >$ 7.4 ppm) than those of the *Z* olefinic protons ($\delta <$ 6.9 ppm).[17] As expected, the ^{1}H NMR spectrum (300 MHz, $CDCl_3$) of **4** shows a pair of doublets (J = 15.9 Hz) at δ = 7.33 and 7.92 ppm for the *E*-olefinic protons and a singlet at δ = 3.88 ppm for the methoxy protons. Similarly, two methyl protons on the pyrene ring are observed as singlets at δ = 2.94 and 2.98 ppm. The structure of compound **4** was also established by the molecular ion at m/z = 418 in its mass spectrum.

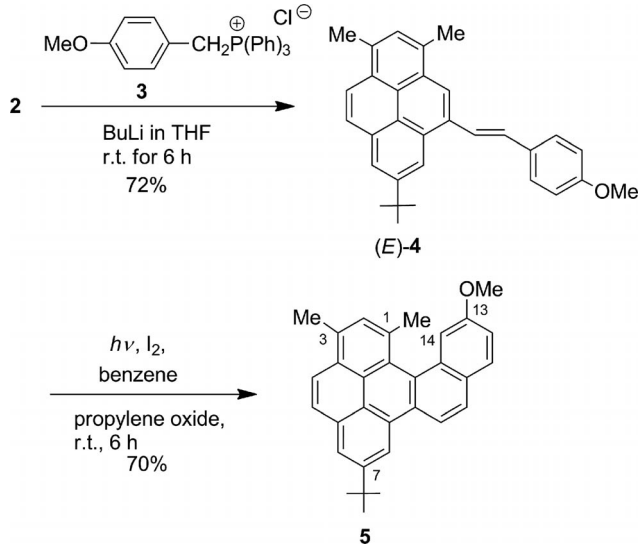

Scheme 2. Synthetic route to 7-*tert*-butly-1,3-dimethyl-13-methoxydibenzo[*ij*,*no*]tetraphene (**5**).

When a solution of (*E*)-**4** (50 mg, 0.12 mmol) and a stoichiometric amount of iodine (31 mg, 0.12 mmol) in benzene (260 mL) was irradiated with a high-pressure mercury lamp (400 W) at room temperature for 6 h, the photocyclized product, 7-*tert*-butyl-1,3-dimethyl-13-methoxydibenzo[*ij*,*no*]-tetraphene (**5**), was obtained in only 10% yield along with recovered starting compound. Prolonging the reaction time

to 12 h led to an increase in the yield to 25%. Irradiation with a stoichiometric amount of iodine plus a large amount of propylene oxide[18,19] (1.53 mL, 21.1 mmol) in the absence of air led to an increase in yield to 70% (Scheme 2).

The structure of product **5** was determined by elemental analyses and spectroscopic data. Its mass spectrum shows a molecular ion at *m*/*z* = 416. The ^{1}H NMR spectrum (300 MHz in $CDCl_3$) of **5** shows a singlet at δ = 1.62 ppm for the *tert*-butyl group, two singlets at δ = 2.50 (1-Me) and 2.97 (3-Me) ppm for two methyl groups, and a singlet at δ = 3.90 ppm for a methoxy group. Compared with the methyl peaks of (*E*)-**4**, the methyl peak at δ = 2.50 ppm for **5** is more shielded by 0.44 ppm. Similarly, the ^{1}H NMR spectrum of compound **5** shows a pair of doublets (J = 9.3 Hz) at δ = 8.70 and 7.69 ppm for 9-H and 10-H, and a pair of doublets (J = 9.0 Hz) at δ = 8.02 and 8.20 ppm for 4-H and 5-H, respectively. A set of characteristic double doublets at δ = 7.22 ppm (dd, J = 2.4, 2.4 Hz) was assigned to 12-H. Similarly, 14-H can clearly be seen to be deshielded at δ = 8.03 ppm by the adjacent rings, a common consequence of extended benzene rings. Furthermore, the helical structure of compound **5** was confirmed by its single-crystal X-ray analysis (see Figure 7).

To investigate this helicity in more detail, two methyl groups were introduced into the fjord regions of the synthesized [4]helicene. An additional methyl group at the 14-position could lead to increased skeletal distortion, even more than that reported in benzo[*c*]phenanthrene.[20] Thus, the reaction of **2** and (3,5-dimethylbenzyl)triphenylphosphonium bromide (**6**) with *n*-butyllithium in THF gave the desired 7-*tert*-butyl-1,3-dimethyl-5-(3,5-dimethylphenylethynyl)pyrene [(*E*)-**7**] in 75% yield (Scheme 3).

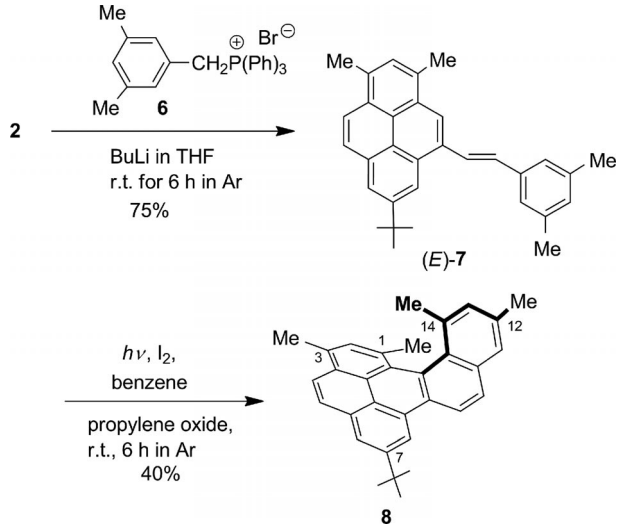

Scheme 3. Synthetic route to 7-*tert*-butly-1,3,12,14-tetramethydibenzo[*ij*,*no*]tetraphene (**8**).

The structure of compound (*E*)-**7** was established by elemental analysis, spectroscopic data, and the molecular ion at *m*/*z* = 416 in its mass spectrum. The ^{1}H NMR spectrum (300 MHz, $CDCl_3$) of (*E*)-**7** shows a singlet at δ = 2.41 ppm for six protons of the methyl groups and two singlets at δ = 2.94 and 2.98 ppm for the two pyrene methyl groups. This NMR spectrum also shows a pair of doublets (J = 15.3 Hz) at δ = 7.30 and 8.01 ppm for the *E*-olefinic protons, which shows the compound to be in the *E* configuration.

When a solution of (*E*)-**7** (50 mg, 0.12 mmol) and a stoichiometric amount of iodine (31 mg, 0.12 mmol) in the presence of propylene oxide (1.53 mL, 21.1 mmol) in benzene (260 mL) was irradiated with a high-pressure mercury lamp (400 W) under the same conditions as described above, the photocyclization product, 7-*tert*-butyl-1,3,12,14-tetramethyldibenzo[*ij*,*no*]tetraphene (**8**), was obtained in 40% yield as a white crystalline solid. The low yield of the compound is a result of the substitution of two methyl groups in the fjord region, which leads to pronounced steric hindrance during the cyclization reaction.

The structure of compound **8** was determined by elemental analysis, spectroscopic data, and the presence of the molecular ion at *m*/*z* = 414 in its mass spectrum. The ^{1}H NMR spectrum (300 MHz, $CDCl_3$) of **8** shows four distinct singlets at δ = 1.82 (14-Me), 2.06 (12-Me), 2.59 (1-Me), and 2.96 (3-Me) ppm for the protons of four methyl groups, two sets of doublets (J = 8.7 Hz) at δ = 7.98 and 8.74 ppm for 10-H and 9-H, and two sets of doublets (J = 9.1 Hz) at δ = 8.04 and 8.21 ppm for 5-H and 4-H, respectively (Figure 2). As expected, the protons of the two methyl groups in the fjord region of the [4]helicene structure are significantly shielded at δ = 1.82 (14-Me) and 2.59 (1-Me) ppm by the adjacent rings, and there is an absence of *meta* coupling in the aromatic protons, a common consequence of the distortion from planarity of peripheral rings.[20]

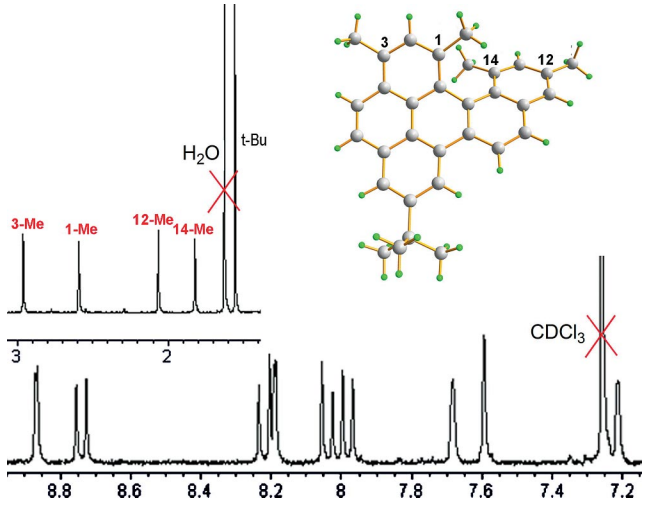

Figure 2. ^{1}H NMR spectra (300 MHz, $CDCl_3$) of **8**.

Photophysical and Electrochemical Properties

The new [4]helicenes **5** and **8** are very soluble in common organic solvents, such as hexane, CH_2Cl_2, $CHCl_3$, and toluene, owing to the presence of the solubilizing *tert*-butyl group. The UV/Vis absorption and fluorescence emission spectra of the [4]helicenes **5** and **8**, and the pre-cyclization products, 7-*tert*-butyl-1,3-dimethyl-5-(phenylethenyl)pyr-

enes **4** and **7**, were recorded in dilute dichloromethane solution at room temperature (Figures 3, 4, and 5). The spectroscopic data are presented in Table 1, together with those of 7-*tert*-butyl-1,3-dimethylpyrene (**1**). The absorption spectrum of 7-*tert*-butyl-1,3-dimethylpyrene (**1**) is almost identical to that of the parent pyrene with three well-resolved, sharp absorption bands observed in the region 300–350 nm. The slight bathochromic shift observed is ascribed to the increased electron density on the pyrene ring arising from the electron-donating nature of the *tert*-butyl and methyl groups at the 7- and 1,3-positions, respectively. The substituted pyrene **1** is more bathochromically redshifted than 2,7-di-*tert*-butylpyrene (**9**)[21] because the alkyl groups are in different positions on the pyrene core and the nodal planes in the HOMO and LUMO of pyrene pass through the 2,7-positions, and thus substitution at the 2,7-positions has a limited effect on the optical properties.[22]

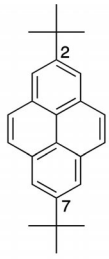

9

The UV/Vis absorption spectra of compounds **4** and **7** (before cyclization) are broad, less well resolved, and the longest-wavelength hyperchromic absorption maxima of **4** and **7** occur at 368 and 373 nm, respectively (Table 1). These are redshifted by 15–19 nm relative to **1** due to the introduction of the phenylethenyl unit at the 5-position leading to an extension of the π conjugation. In addition, of these compounds, the 3,5-dialkyl-substituted phenylethenyl pyrene **7** displays a slightly greater bathochromic shift (ca. 5 nm) compared to the (4-methoxyphenylethenyl)pyrene **4**, which can be attributed to the stronger electron-donating nature of the two alkyl groups than that of the methoxy group.

The UV spectra of the dibenzo[*ij*,*no*]tetraphene derivatives **5** and **8** are almost identical, with the absorption bands observed in the range of 300–410 nm (Figure 3). However, the quite different shapes of the UV spectra of **4** and **7**, and the UV spectra of **5** and **8** can be ascribed to the differences in the π-conjugation systems caused by the cyclization reaction. The pronounced hypochromic absorption of the absorption bands at 350–400 nm can be ascribed to the absence of the phenylethenyl unit, the decrease in aromaticity, the increase in distortions from planarity, and, consequently, the decrease in π conjugation after cyclization. The UV spectra of **5** and **8** in CH_2Cl_2 show a large number of transition bands (Figure 3), typical of PAHs.[23]

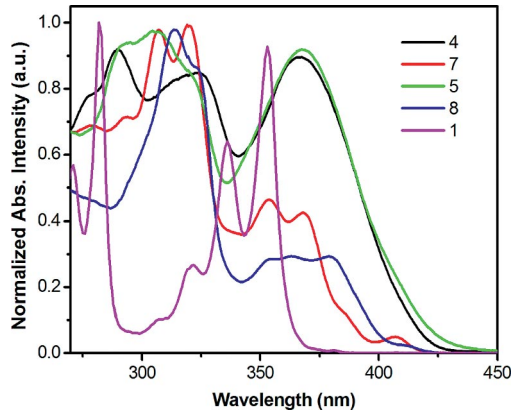

Figure 3. Normalized UV/Vis absorption spectra of **4** and **7** (before cyclization), and **5** and **8** (after cyclization), and, for comparison, **1**, recorded at a concentration of ca. 10^{-5} M at room temperature.

The absorption band at 404 nm for **5** due to the methoxy group also indicates a departure of the aromatic rings from planarity. On the other hand, the different shape of the UV spectrum of **8** confirms the increase in the nonplanarity of the aromatic rings to avoid steric crowding by overlapping methyl groups at C-1 and C-14.

Upon excitation, dilute solutions (ca. 10^{-6} M) of compounds **4**, **7**, and **1** in dichloromethane at room temperature show a broad blue emission band (Figures 4 and 5). Compared with the emission band of 7-*tert*-butyl-1,3-dimethylpyrene (**1**) at 403 nm, the emission bands of **4** and **7** are redshifted to 433 and 455 nm, respectively. Both compounds were observed in the visible pure-blue region. All the fluorescence emission bands are broad but not identical; the emission band of **4** shows a small shoulder at 452 nm. The emission band of compound **7** is broad but only slightly redshifted (ca. 22 nm) compared with **4**, which has been ascribed to the high alkyl substitution in the compound, and therefore **7** exhibits a higher Stokes shift than **4**.

Table 1. Photophysical and electrochemical data for **1**, **4**, **7**, **5**, and **8**.

	λ_{max} abs [nm]		λ_{max} PL [nm][c]		Stokes shift [nm]		Φ_f[d]	E_g[e]	HOMO[f]	LUMO[g]
	Soln.[a]	Film[b]	Soln.[a]	Film[b]	Soln.[a]	Film[b]	Soln./thin film/doped film	[eV]	[eV]	[eV]
1	353	n.d.	403 (222)	n.d.	50	n.d.	0.09/n.d./n.d.	n.d.	n.d.	n.d.
4	368	n.d.	433 (222)	n.d.	65	n.d.	0.77/n.d./n.d.	n.d.	n.d.	n.d.
7	373	n.d.	455 (221)	n.d.	83	n.d.	0.88/n.d./n.d.	n.d.	n.d.	n.d.
5	371	370	419 (220)	414 (320)	48	44	0.11/0.08/0.10	3.12	–5.76	–2.64
8	382	381	422 (219)	450 (315)	40	69	0.13/0.07/0.12	3.04	–5.72	–2.68

[a] Measured in dichloromethane at room temperature. [b] Measured in thin neat films. n.d.: not detected. [c] PL: photoluminescence. The values in parentheses are the excitation wavelengths. [d] Measured in dichloromethane, thin neat films, and 1 wt.-% doped poly(methyl methacrylate) (PMMA) films. [e] Optical band gap estimated from the onset point (onset) of the absorption band of the thin film: $E_g = 1240/\lambda_{onset}$. [f] Calculated from the oxidation potentials. [g] Calculated from the HOMO energy levels and E_g.

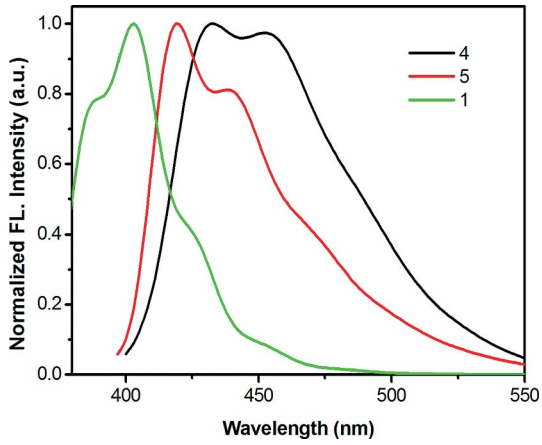

Figure 4. Normalized fluorescence spectra of **4** (before cyclization) and **5** (after cyclization), and, for comparison, **1**, recorded at a concentration of ca. 10^{-6} M at room temperature.

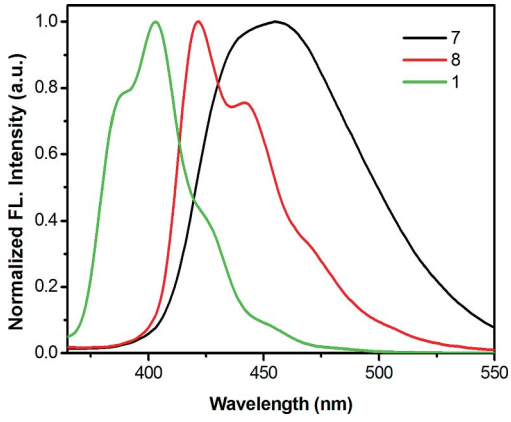

Figure 5. Normalized fluorescence spectra of **7** (before cyclization) and **8** (after cyclization), and, for comparison, **1**, recorded at ca. 10^{-6} M concentration room temperature, compared with that of **1**.

The emission spectra of compounds **5** and **8** (after cyclization) in CH_2Cl_2 are also shown in Figure 4 and Figure 5, and the data are presented in Table 1. Compared with the band of **1**, the bands (major) of **5** and **8** at 419 and 422 nm, respectively, are redshifted. The fluorescence emission bands are sharper than those of the starting compounds **4** and **7** with a small shoulder at longer wavelength.

Remarkably high quantum yields are observed for compounds **4** and **7** because of greater π conjugation along the phenylethenyl unit at the 5-position in the pyrene ring (Table 1). The high fluorescence quantum yields of **4** and **7** are due to the electron-donating groups attached to the phenylethenyl unit. The fluorescence quantum yields of **5** and **8** are low compared with those of **4** and **7** because of low aromaticity after cyclization and consequently lower electron delocalization around the aromatic core. Although the shift is not pronounced, the maximum emission bands of **5** and **8** are less redshifted compared with those of **4** and **7**. The less redsifted values of **5** and **8** are due to the substituted groups causing a loss of co-planarity after cyclization. On the other hand, the different structural characteristics of the compounds after cyclization are clearly observed in emission spectra. Upon excitation, the emission band of 2,7-di-*tert*-butyldibenzo[*ij*,*no*]tetraphenes (**10**)[21] are redshifted in comparison with cyclized **5** and **8**; the considerable hypsochromic blueshift of **5** and **8** is ascribed to their more twisted structure.

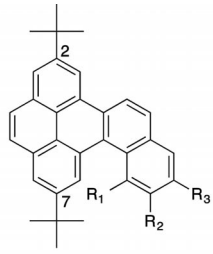

10 **a**: $R_1 = R_2 = R_3 = H$
b: $R_1 = R_3 = H$, $R_2 = OMe$
c: $R_1 = R_3 = Me$, $R_2 = H$

The normalized UV/Vis absorption spectra and emission spectra of **5** and **8** in thin neat films are shown in Figure S3–1 in the Supporting Information, and the spectroscopic data are summarized in Table 1. In the UV spectra of both **5** and **8**, a small hypsochromic shift (ca. 1 nm) is observed relative to the corresponding spectra in solution, which indicates that these two compounds have similar conformations in both states.[24] Interestingly, compared with their corresponding spectra in solution, the photoluminescence spectra of **5** and **8** show a main emission peak at 414 nm with a small hypsochromic shift (ca. 5 nm) for **5** and a main emission peak at 450 nm with a large bathochromic shift (ca. 28 nm) for **8**, respectively. However, no excimer emission is observed in the emission spectra of **5** and **8** owing to their twisted molecular structures after cyclization (see Figure S3–1). We also examined the fluorescence emission spectra of thin films of poly(methyl methacrylate) (PMMA) doped with 1 wt.-% **5** and **8**.[25] The spectra each show deep-blue emission with a maximum peak at 414 and 419 nm for **5** and **8**, respectively (Figure 6), almost identical to the corresponding emissions in solution, which indicates that the π stacking of the pyrene units may be inhibited in doped films. These results suggest that these newly developed pyr-

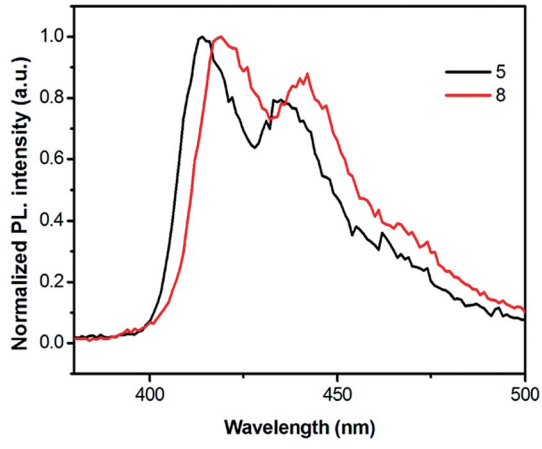

Figure 6. Emission spectra of thin films of PMMA doped with 1 wt.-% **5** and **8**.

ene-based [4]helicenes **5** and **8** might be promising candidates in deep-blue organic light-emitting diodes (OLEDs).[26]

The fluorescence quantum yields of **4**, **7**, **5**, and **8** recorded in dilute dichloromethane solutions and thin films are also listed in Table 1, together with those of **1**. The Φ_f values of the cyclized [4]helicenes **5** and **8** are moderate, ranging from 0.07 to 0.13, whereas the Φ_f values of the pre-cyclization products **4** and **7** are quite high, ranging from 0.77 to 0.88. The low quantum yields obtained in solution and in thin films for the [4]helicenes **5** and **8** indicate that excitons are not confined to the backbone of these molecules due to their non-planar twisted molecular structures; some energy loss may occur during the exciton migrations,[27] thereby resulting in low quantum yields. However, the high fluorescence quantum yields for the pre-cyclization products **4** and **7** in solution indicate that the excitons are completely confined to the backbone of **4** and **7**, arising from the extended π-delocalization between the rigid phenylethenyl groups and the central pyrene core, thereby giving higher quantum yields.

To investigate the redox behavior of these new [4]helicenes and estimate their frontier molecular orbital levels we carried out cyclic voltammetry (CV) experiments on **5** and **8** by using a conventional three-electrode cell with 0.1 M tetrabutylammonium hexafluorophosphate (Bu_4NPF_6) as supporting electrolyte in dichloromethane and ferrocene as the internal standard. The cyclic voltammograms are shown in Figure S4–1 in the Supporting Information. Both **5** and **8** exhibit one reversible oxidation process in the anodic sweep, but no reduction signal was detected for either of these [4]helicenes during the cathodic scan. As shown in Figure S4–1, the oxidation wave of **8** is shifted to a less positive potential compared with that of **5**. This implies that the removal of the first electron from **8** is easier than from **5**. The half-potentials ($E^{1/2}$) of the first oxidation waves are 1.36 and 1.32 V, respectively, relative to ferrocene. The HOMO energy levels were estimated according to the equation of HOMO = –($E^{1/2}$ + 4.4 eV) to be –5.76 and –5.72 eV for **5** and **8**, respectively.[28] These values further indicate that these [4]helicenes are potential deep-blue emitters for optoelectronic device applications such as OLEDs.[29] The energies of the band gaps were determined by the absorption edge technique,[28] and the LUMO levels calculated by subtracting the gap from the energy of the HOMO. The electrochemical and electronic data for **5** and **8** are presented in Table 1.

X-ray Molecular Structures

To investigate the molecular structures of the newly developed pyrene-based [4]helicenes in the solid state, we obtained suitable crystals of **5** and **8** by vapor diffusion of hexane into their dichloromethane solutions. The crystallographic data for compounds **5** and **8** are summarized in the Exp. Sect. and in Table S1 in the Supporting Information.[30] The molecular geometry of the helical skeleton of the helicene **5** (Figure 7) contains long and short C–C bonds. The longer bonds are those mostly affected by intramolecular torsion (namely C3–C4, C4–C11, C11–C12, C12–C27), with an average of 1.43 Å. Note that in the peripheral rings, the C8–C9 bond length [1.363(4) Å] is significantly shorter than its counterpart C4–C11 [1.461(4) Å], which experiences more twisting to reduce steric hindrance with the more rigid pyrene core. The torsion angles along the inner helical rim of the fjord region C27–C12–C11–C4 and C12–C11–C4–C3 are –18.5(5) and –21.5(5)°, respectively. Nonbonding distances [Å] were calculated to be 5.951 Å for C30–O1, 5.397 Å for C27–C2, and 2.991 Å for C12–C6. These values are also a convenient measure of the helicity.[9]

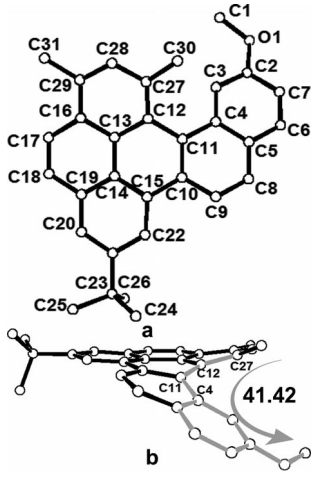

Figure 7. X-ray structure of compound **5**.

A similar molecular geometry is observed for the helical skeleton of **8** with the corresponding torsion angles along the inner helical rim of the fjord region C13–C12–C11–C33 and C12–C11–C33–C32 being 21.8(3) and 33.2(3)°, respectively (Figure 8). These values indicate a more twisted conformation due to the bulkier Me groups at C13 and C32 in **8** (Figure 8, b, 47.83°) compared with those of the H atoms at C3 and C27 in **5** (Figure 7, b, 41.42°).

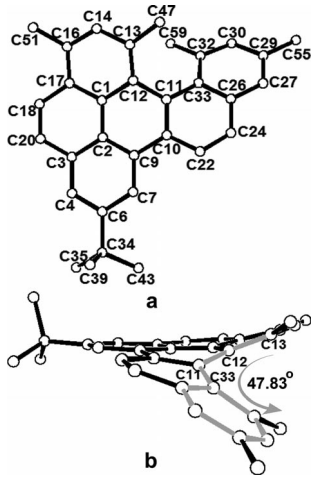

Figure 8. X-ray structure of compound **8**.

Conclusions

The formylation of 7-*tert*-butyl-1,3-dimethylpyrene (**1**) with dichloromethyl methyl ether in the presence of $TiCl_4$ successfully afforded 7-*tert*-butyl-1,3-dimethylpyrene-5-carbaldehyde (**2**). Wittig reaction of the 5-formylated pyrene **2** with (4-methoxybenzyl)triphenylphosphonium chloride and (3,5-dimethylbenzyl)triphenylphosphonium bromide gave the corresponding arylethenylpyrenes **4** and **7**. Photoinduced intramolecular cyclization of these arylethenylpyrenes in the presence of iodine and propylene oxide led to the corresponding dibenzo[*ij*,*no*]tetraphene derivatives **5** and **8** containing methyl groups in the fjord region. As expected, the presence of two methyl groups in the fjord region of the [4]helicene **8** gives a more distorted structure. The photophysical and electrochemical properties of these compounds were fully examined in solution and in thin films. Further studies on the chemical and physical properties of the new class of pyrene-based [4]helicenes are now in progress.

Experimental Section

General: ^{1}H NMR spectra were recorded with a Nippon Denshi JEOL FT-300 spectrometer. Chemical shifts are reported as δ values (ppm) relative to internal Me_4Si. IR spectra were recorded as KBr pellets with a Nippon Denshi JIR-AQ2OM spectrometer. UV/Vis spectra were recorded with a Perkin–Elmer Lambda 19 UV/Vis/NIR spectrophotometer in various organic solvents. Fluorescence spectroscopic studies were performed in various organic solvents in a semimicro fluorescence cell (Hellma®, 104F-QS, 10 × 4 mm, 1400 μL) with a Varian Cary Eclipse spectrophotometer. Fluorescence quantum yields were determined by using absolute methods. Mass spectra were obtained with a Nippon Denshi JMS-HX110A Ultrahigh Performance mass spectrometer at 75 eV by using a direct-inlet system. Elemental analyses were performed with a Yanaco MT-5 analyzer. GLC analyses were performed by using a Shimadzu GC-14A gas chromatograph (silicone OV-1, 2 m; programmed temperature rise, 12 °C min^{-1}; nitrogen carrier gas, 25 mL min^{-1}). Electrochemical properties and the HOMO and LUMO energy levels were determined by using an Electrochemical Analyzer.

The preparation of 7-*tert*-butyl-1,3-dimethylpyrene (**1**) has been described previously.[15,16]

7-*tert*-Butyl-1,3-dimethylpyrene-5-carbaldehyde (2): A solution of titanium tetrachloride (0.10 mL, 0.91 mmol) in CH_2Cl_2 (1 mL) was added to a stirred solution of **1** (106 mg, 0.37 mmol) and dichloromethyl methyl ether (74 mg, 0.64 mmol) in CH_2Cl_2 (5 mL) at 0 °C. This mixture was stirred for 2 h at room temperature. The mixture was poured into a large amount of ice/water and extracted with CH_2Cl_2 (2 × 25 mL). The combined organic layers were washed with water (2 × 25 mL), dried with $MgSO_4$, and concentrated under reduced pressure. The residue was recrystallized from hexane to afford **2** as pale-yellow prisms (80 mg, 69%); m.p. 268–269 °C. IR (KBr): $\tilde{\nu}_{max}$ = 2964, 2946, 1671 (C=O), 1589, 1503, 1471, 1460, 1363, 1231, 1163, 898, 747, 472, 422 cm^{-1}. ^{1}H NMR (300 MHz, $CDCl_3$): δ = 1.62 (s, 9 H, *t*Bu), 2.93 (s, 3 H, Me), 2.95 (s, 3 H, Me), 7.69 (s, 1 H, 2-H_{Py}), 8.02 (d, J = 9.2 Hz, 1 H, 9-H_{Py}), 8.12 (d, J = 9.2 Hz, 1 H, 10-H_{Py}), 8.25 (d, J = 2.0 Hz, 1 H, 8-H_{Py}), 8.61 (s, 1 H, 4-H_{Py}), 9.73 (d, J = 2.0 Hz, 1 H, 6-H_{Py}), 10.49 (s, 1 H, CHO) ppm. HRMS (FAB, EI): calcd. for $C_{31}H_{30}O$ [M]$^+$ 314.1671; found 314.1670. $C_{23}H_{22}O$ (314.42): calcd. C 87.86, H 7.05; found C 87.85, H 7.06.

7-*tert*-Butyl-1,3-dimethyl-5-(4-methoxyphenylethenyl)pyrene [(*E*)-4]: The Wittig reagent was prepared from triphenylphosphane and 4-methoxybenzyl chloride in dry benzene. *n*-Butyllithium in hexane (1.20 mL, 1.89 mmol) was slowly added to a solution of this Wittig reagent (794 mg, 1.89 mmol) in dry THF (15 mL) at 0 °C under argon. The mixture was stirred for 10 min and a solution of **2** (200 mg, 0.632 mmol) in dry THF (15 mL) was injected under the same conditions. After the addition, the mixture was warmed to room temperature, stirring for 6 h under argon. The mixture was quenched by a large amount of ice/water and extracted with ethyl acetate (2 × 100 mL). The combined extracts were washed with water, dried with $MgSO_4$, and concentrated. The residue was purified by column chromatography over silica gel (Wako C-300, 200 g) with hexane/dichloromethane (5:1) as eluent to give (*E*)-**4** (NMR analysis) as a light-yellow solid. Recrystallization from hexane/dichloromethane (5:1, v/v) afforded the *anti* compound (*E*)-**4** (190 mg, 72%); m.p. 150–152 °C. IR (KBr): $\tilde{\nu}_{max}$ = 2961, 1601, 1504, 1455, 1247, 1171, 1025, 956, 880, 804, 565 cm^{-1}. ^{1}H NMR (300 MHz, $CDCl_3$): δ = 1.59 (s, 9 H, *t*Bu), 2.94 (s, 3 H, *Me*), 2.98 (s, 3 H, Me), 3.88 (s, 3 H, OMe), 7.00 (d, J = 8.7 Hz, 2 H, Ar-H), 7.33 (d, J = 15.9 Hz, 1 H, -CH=CH_a-), 7.65 (d, J = 8.7 Hz, 2 H, Ar-H), 7.70 (s, 1 H, 2-H_{Py}), 7.92 (d, J = 15.9 Hz, 1 H, -CH_b=CH-), 8.02 (d, J = 9.0 Hz, 1 H, 9-H_{Py}), 8.18 (d, J = 9.0 Hz, 1 H, 10-H_{Py}), 8.21 (d, J = 1.8 Hz, 1 H, 8-H_{Py}), 8.36 (s, 1 H, 4-H_{Py}), 8.48 (d, 1 H, J = 1.8 Hz, 6-H_{Py}) ppm. ^{13}C NMR (75 MHz, $CDCl_3$): δ = 19.7, 32.0, 35.3, 55.4, 114.2, 118.4, 121.1, 122.2, 123.5, 125.1, 126.5, 127.4, 127.5, 128.0, 130.0, 130.7, 131.2, 131.5, 131.8, 133.6, 148.5, 159.4 ppm. HRMS (FAB, EI): calcd. for $C_{31}H_{30}O$ [M]$^+$ 418.2297; found 418.2299. $C_{31}H_{30}O$ (418.57): calcd. C 88.95, H 7.22; found C 88.96, H 7.20.

7-*tert*-Butyl-1,3-dimethyl-5-(3,5-dimethylphenylethenyl)pyrene [(*E*)-7]: The Wittig reagent was prepared from triphenylphosphane and 3,5-dimethylbenzyl bromide in dry benzene. *n*-Butyllithium in hexane (0.933 mL, 1.50 mmol) was slowly added to a solution of this Wittig reagent (692 mg, 1.50 mmol) in dry THF (15 mL) at 0 °C under argon. The mixture was stirred for 10 min and the solution of **2** (316 mg, 1 mmol) in dry THF (20 mL) was injected under the same conditions. After the addition, the mixture was warmed to room temperature, stirring for 6 h under argon. The mixture was quenched by a large amount of ice/water and extracted with ethyl acetate (2 × 100 mL). The combined extracts were washed with water, dried with $MgSO_4$, and concentrated. The residue was purified by column chromatography over silica gel (Wako C-300, 200 g) with hexane/ethyl acetate (5:1) as eluent to give (*E*)-**7** (^{1}H NMR analysis) as a light-yellow solid. Recrystallization from hexane/toluene (2:1) and washing with hexane afforded the *anti* compound (*E*)-**7** (215 mg, 75%); m.p. 106 °C. IR (KBr): $\tilde{\nu}_{max}$ = 2961, 1603, 1478, 1460, 1360, 1206, 1106, 1016, 873, 805, 472 cm^{-1}. ^{1}H NMR (300 MHz, $CDCl_3$): δ = 1.59 (s, 9 H, *t*Bu), 2.41 (s, 6 H, Ar-*Me*), 2.94 (s, 3 H, Py-*Me*), 2.98 (s, 3 H, Py-*Me*), 7.00 (s, 2 H, Ar-H), 7.30 (d, J = 15.3 Hz, 1 H, -CH=CH_a-), 7.33 (s, 1 H, Ar-H), 7.70 (s, 1 H, 2-H_{Py}), 8.01 (d, J = 15.3 Hz, 1 H, -CH_b=CH-), 8.05 (d, J = 9.0 Hz, 1 H, 9-H_{Py}), 8.18 (d, J = 9.0 Hz, 1 H, 10-H_{Py}), 8.21 (d, J = 1.8 Hz, 1 H, 8-H_{Py}), 8.36 (s, 1 H, 4-H_{Py}), 8.48 (d, 1 H, J = 1.8 Hz, 6-H_{Py}) ppm. ^{13}C NMR (75 MHz, $CDCl_3$): δ = 21.4, 30.9, 32.0, 35.4, 118.5, 121.5, 122.2, 123.5, 124.7, 126.6, 126.9, 127.4, 129.6, 129.9, 130.0, 131.4, 131.6, 131.9, 132.0, 133.7, 137.8, 138.3, 148.5 ppm. HRMS (FAB, EI): calcd. for $C_{32}H_{32}$ [M]$^+$ 416.2504; found 416.2496. $C_{32}H_{32}$ (416.60): calcd. C 92.26, H 7.14; found C 92.27, H 7.13.

General Procedure for Photocyclization: The photoreactor was a cylindrical glass vessel with an immersion well and two tapered joints. A vertical joint was attached to a condenser to which an argon source was fitted. The other joint was angled for withdrawal and addition of samples. The vessel was flat-bottomed to allow a magnetic stirring bar to rotate. The immersion well was a double-walled Pyrex tube cooled by water and containing a high-pressure quartz Hg vapor lamp. Argon gas was bubbled through benzene for 20–30 min, which was used to dissolve the sample and iodine. The solution of pyrene, iodine, and propylene oxide was added to the reaction vessel through the angled joint and the lamp was switched on. The reaction was carried out under argon. The photoreactions were monitored by ^{1}H NMR spectroscopy and the change in color of the iodine. After complete irradiation, work-up was performed which included washing with 15% $Na_2S_2O_3 \cdot H_2O$ and saturated brine, drying with anhydrous $MgSO_4$, filtering, and concentration to dryness on a rotary evaporator. The residue obtained was either washed through a short column of silica gel or different solvent systems were used to obtain the pure compounds.

7-*tert*-Butyl-1,3-dimethyl-13-methoxydibenzo[*ij*,*no*]tetraphene (5): 7-*tert*-Butyl-1,3-dimethyl-5-(4-methoxyphenylethenyl)pyrene [(*E*)-**4**, 50 mg, 0.12 mmol] in benzene (260 mL) was irradiated in the presence of I_2 (31 mg, 0.12 mmol) and propylene oxide (1.53 mL, 21.1 mmol) for 6 h. Following work-up, the mixture was adsorbed on silica gel by using dichloromethane and purified by column chromatography with hexane as eluent. The viscous material obtained from the column was dissolved in diethyl ether and left overnight to leave a white solid. The compound was further recrystallized from diethyl ether and washed with hot hexane to afford **5** as a white solid (34 mg, 70%); m.p. 140–141 °C. IR (KBr): $\tilde{\nu}_{max}$ = 2953, 2919, 1603, 1458, 1452, 1373, 1217, 1102, 1035, 875, 755, 675, 472 cm^{-1}. ^{1}H NMR (300 MHz, $CDCl_3$): δ = 1.62 (s, 9 H, *t*Bu), 2.50 (s, 3 H, 1-Me), 2.97 (s, 3 H, 3-Me), 3.90 (s, 3 H, OMe), 7.22 (dd, J = 2.4, 2.4 Hz, 1 H, 12-H_{Ar}), 7.50 (s, 1 H, 2-H_{Ar}), 7.69 (d, J = 9.3 Hz, 1 H, 10-H_{Ar}), 7.90 (d, J = 9.0 Hz, 1 H, 11-H_{Ar}), 8.02 (d, J = 9.0 Hz, 1 H, 5-H_{Ar}), 8.03 (s, 1 H, 14-H_{Ar}), 8.17 (d, J = 1.8 Hz, 1 H, 6-H_{Ar}), 8.20 (d, J = 9.0 Hz, 1 H, 4-H_{Ar}), 8.70 (d, J = 9.3 Hz, 1 H, 9-H_{Ar}), 8.89 (d, J = 1.8 Hz, 1 H, 8-H_{Ar}) ppm. ^{13}C NMR (75 MHz, $CDCl_3$): δ = 19.4, 25.1, 31.9, 35.4, 55.2, 107.8, 109.2, 113.7, 115.4, 117.1, 117.9, 118.5, 122.8, 123.0, 126.1, 126.8, 127.1, 127.6, 128.9, 130.3, 130.9, 131.9, 132.3, 133.3, 148.7, 157.6 ppm. HRMS (FAB, EI): calcd. for $C_{31}H_{28}O$ [M]$^+$ 416.2140; found 416.2148. $C_{31}H_{28}O$ (416.55): calcd. C 89.38, H 6.78; found C 89.39, H 6.76. The structure of **5** was supported by single-crystal X-ray structure analysis.

7-*tert*-Butyl-1,3,12,14-tetramethyldibenzo[*ij*,*no*]tetraphene (8): 7-*tert*-Butyl-1,3-dimethyl-5-(3,5-dimethylphenylethynyl)pyrene [(*E*)-**7**; 50 mg, 0.12 mmol] in benzene (260 mL) was irradiated in the presence of I_2 (31 mg, 0.12 mmol) and propylene oxide (1.53 mL, 21.1 mmol) for 10 h. Following work-up, the mixture was adsorbed on silica gel by using dichloromethane and purified by column chromatography with hexane as eluent to give pure **8** as a white crystalline solid (20 mg, 40%); m.p. 165–166 °C. IR (KBr): $\tilde{\nu}_{max}$ = 2953, 2919, 1600, 1457, 1442, 1363, 1217, 1102, 1034, 873, 751, 665, 472 cm^{-1}. ^{1}H NMR (300 MHz, $CDCl_3$): δ = 1.62 (s, 9 H, *t*Bu), 1.82 (s, 3 H, 14-Me), 2.06 (s, 3 H, 12-Me), 2.59 (s, 3 H, 1-Me), 2.96 (s, 3 H, 3-Me), 7.21(s, 1 H, 13-H_{Ar}), 7.59 (s, 1 H, 11-H_{Ar}) 7.68 (s, 1 H, 2-H_{Ar}), 7.98 (d, J = 8.7 Hz, 1 H, 10-H_{Ar}), 8.04 (d, J = 9.1 Hz, 1 H, 5-H_{Ar}), 8.19 (d, J = 1.5 Hz, 1 H, 6-H_{Ar}), 8.21 (d, J = 9.1 Hz, 1 H, 4-H_{Ar}), 8.74 (d, J = 8.4 Hz, 1 H, 9-H_{Ar}), 8.86 (d, J = 1.5 Hz, 1 H, 8-H_{Ar}) ppm. ^{13}C NMR (75 MHz, $CDCl_3$): δ = 19.5, 21.4, 23.3, 23.3, 31.9, 35.4, 117.6, 119.7, 122.3, 123.2, 124.7, 126.0, 126.7, 127.2, 127.3, 128.9, 130.3, 130.6, 130.7, 130.8, 131.1, 131.9, 133.0, 134.4, 135.2, 136.4, 146.9, 148.7 ppm. HRMS (FAB, EI): calcd. for $C_{32}H_{30}$ [M]$^+$ 414.2347; found 414.2356. $C_{32}H_{32}$ (414.58): calcd. C 92.71, H 7.29; found C 92.70, H 7.30. The structure of **8** was supported by single-crystal X-ray structure analysis.

Crystallographic Data of 5 and 8[30]

Crystal Data for 5: $C_{31}H_{28}O$, M_r = 416.53, monoclinic, $P2_1/c$, a = 30.160(2), b = 5.8496(3), c = 25.6873(14) Å, β = 101.737(3)°, V = 4437.1(4) Å^3, Z = 8, D_c = 1.247 g cm^{-3}, μ(Mo-K_α) = 0.073 mm^{-1}, T = 150(2) K, colorless lath; 125835 reflections measured with a Nonius–Kappa CCD diffractometer, of which 8336 are independent; data corrected for absorption on the basis of symmetry equivalent and repeated data (min. and max. transmission factors: 0.988 and 0.997) and Lorentzian and polarization effects, R_{int} = 0.0776, structure solved by direct methods (Sir2002),[31] F^2 refinement, R_1 = 0.0633 for 4000 data with $F^2 > 2\sigma(F^2)$, wR_2 = 0.1692 for all data, 614 parameters. There are two molecules in the asymmetric unit, one of which was modeled with two-fold disorder of the methyl groups in the *i*Bu group containing C54 (in the asymmetric unit of the second molecule, not shown in Figure 7).

Crystal Data for 8: $C_{32}H_{30}$, M_r = 414.56, triclinic, $P\bar{1}$, a = 8.2687(5), b = 8.4703(5), c = 16.9751(11) Å, α = 98.2723(9), β = 91.1145(9), γ = 110.5735(9)°, V = 1098.35(12) Å^3, Z = 2, D_c = 1.253 g cm^{-3}, μ(Mo-K_α) = 0.073 mm^{-1}, T = 150(2) K, yellow tablet; 17374 reflections measured with a Bruker APEX II CCD diffractometer, of which 6783 are independent; data corrected for absorption on the basis of symmetry equivalent and repeated data (min. and max. transmission factors: 0.937, 0.993) and Lorentzian and polarization effects, R_{int} = 0.022, structure solved by direct methods (SHELXS-97),[32] F^2 refinement, R_1 = 0.049 for 5638 data with $F^2 > 2\sigma(F^2)$, wR_2 = 0.146 for all data, 409 parameters.

Supporting Information (see footnote on the first page of this article): ^{1}H and ^{13}C NMR spectra of **4**, **5**, **7**, and **8**, packing diagrams of **5** and **8**, normalized UV/Vis absorption and emission spectra of **5** and **8** recorded in thin neat films, cyclic voltammograms of **5** and **8**, and summary of the crystal data of **5** and **8**.

Acknowledgments

This work was performed under the Cooperative Research Program of "Network Joint Research Center for Materials and Devices", Institute of Materials Chemistry and Engineering, Kyushu University. The authors would like to thank the Ocean Thermal Energy Conversion (OTEC) at Saga University for financial support.

[1] a) R. Weitzenbock, H. Lieb, *Monatsh. Chem.* **1912**, *33*, 549–565; b) R. Weitzenbock, A. Klinger, *Monatsh. Chem.* **1918**, *39*, 315–324; c) F. Mayer, T. Oppenheimer, *Ber. Dtsch. Chem. Ges.* **1918**, *51*, 510–516; d) F. Mayer, T. Oppenheimer, *J. Chem. Soc.* **1918**, *114i*, 339–340.
[2] J. W. Cook, *J. Chem. Soc.* **1931**, 2524–2528.
[3] J. W. Cook, C. L. Heweit, *J. Chem. Soc.* **1933**, 549–565.
[4] a) G. Portella, J. Poater, J. M. Bofill, P. Alemany, M. Sola, *J. Org. Chem.* **2005**, *70*, 2509–2521; b) H. Hopf, *Classical Hydrocarbon Chemistry*, Wiley-VCH, Weinheim, Germany, **2000**, chapter 12.
[5] F. L. Hirshfeld, S. Sandler, G. M. J. Schmidt, *J. Am. Chem. Soc.* **1963**, *85*, 2108–2125.
[6] S. S. Hecht, A. A. Melikian, S. Amin, in: *Polycyclic aromatic hydrocarbon carcinogenesis: Structure-Activity Relationships*, CRC Press, Boca Raton, FL, **1988**, vol. 1, chapter 4.
[7] D. M. Jerina, J. M. Sayer, H. Yagi, M. Croisy-Delcey, Y. Ittah, D. R. Thakker, A. W. Wood, R. L Chang, W. Levin, in: *Bio-*

logical Reactive Intermediates II, *Part A*, Plenum Press, New York, **1982**, p. 501–523.

[8] a) M. S. Newman, *J. Am. Chem. Soc.* **1940**, *62*, 1683–1687; b) M. S. Newman, *J. Am. Chem. Soc.* **1940**, *62*, 2295−2300.

[9] M. K. Lakshman, P. L. Kole, S. Chaturvedi, J. H. Saugier, H. J. C. Yeh, J. P. Glusker, H. K. Carrell, A. K. Katz, C. E. Afshar, W.-M. Dashwood, G. Kenniston, W. M. Baird, *J. Am. Chem. Soc.* **2000**, *122*, 12629–12636.

[10] H. Goto, K. Akagi, *Angew. Chem.* **2005**, *117*, 4396; *Angew. Chem. Int. Ed.* **2005**, *44*, 4322–4328.

[11] J. Szeliga, A. Dipple, *Chem. Res. Toxicol.* **1998**, *11*, 1–11.

[12] a) S. Amin, J. Camanzo, K. Huie, S. S. Hecht, *J. Org. Chem.* **1984**, *49*, 381–384; b) C. M. Utermoehlen, M. Singh, R. E. J. Lehr, *J. Org. Chem.* **1987**, *52*, 5574–5582; c) S. Amin, G. Balanikas, K. Huie, S. S. Hecht, *Chem. Res. Toxicol.* **1988**, *1*, 349–355; d) B. Mishra, S. Amin, *J. Org. Chem.* **1990**, *55*, 4478–4480.

[13] E. Clar, *Polycyclic hydrocarbons*, Academic Press, New York, **1964**, vol II.

[14] M. Minabe, S. Takeshige, Y. Soeda, T. Kimura, M. Tsubata, *Bull. Chem. Soc. Jpn.* **1994**, *67*, 172–179.

[15] T. Yamato, A. Miyazawa, M. Tashiro, *J. Chem. Soc. Perkin Trans. 1* **1993**, 3127–3137.

[16] T. Yamato, J.-Y. Hu, *J. Chem. Res.* **2006**, 762–765.

[17] A. Merz, A. Karl, T. Futterer, N. Stacherdinger, O. Schneider, J. Lex, E. Lubochand, J. F. Biernt, *Liebigs Ann. Chem.* **1994**, 1199–1209.

[18] L. Liu, B. Yang, T. J. Katz, M. K. Piondexter, *J. Org. Chem.* **1991**, *56*, 3769–3775.

[19] I. Ben, L. Castedo, J. M. Saa, J. A. Seijas, R. Suau, G. Tojo, *J. Org. Chem.* **1985**, *50*, 2236–2240.

[20] C. Brule, K. K. Laali, T. Okazaki, M. K. Lakshman, *J. Org. Chem.* **2007**, *72*, 3232–3241.

[21] a) A. Paudel, J.-Y. Hu, T. Yamato, *J. Chem. Res.* **2008**, 457–460; b) J.-Y. Hu, A. Paudel, N. Seto, X. Feng, M. Era, T. Matsumoto, J. Tanaka, M. R. J. Elsegood, C. Redshaw, T. Yamato, *Org. Biomol. Chem.* **2013**, *11*, 2186–2197; c) X. Feng, J.-Y. Hu, F. Iwanaga, N. Seto, C. Redshaw, M. R. J. Elsegood, T. Yamato, *Org. Lett.* **2013**, *15*, 1318–1321.

[22] A. G. Crawford, A. D. Dwyer, Z.-Q. Liu, A. Steffen, A. Beeby, L.-O. Pålsson, D. L. Tozer, T. B. Marder, *J. Am. Chem. Soc.* **2011**, *133*, 13349–13362.

[23] D. Wasserfallen, M. Kastler, W. Pisula, W. A. Hofer, Y. Borgel, Z. Wang, K. Mullen, *J. Am. Chem. Soc.* **2006**, *128*, 1334–1339.

[24] S. Chen, X. Xu, Y. Liu, G. Yu, X. Sun, W. Qiu, Y. Ma, D. Zhu, *Adv. Funct. Mater.* **2005**, *15*, 1541–1546.

[25] K. D. Singer, J. E. Sohn, S. J. Lalama, *Appl. Phys. Lett.* **1986**, *49*, 248–250.

[26] L. Shi, Z. Liu, G. Dong, L. Duan, Y. Qiu, J. Jia, W. Guo, D. Zhao, D. Cui, X. Tao, *Chem. Eur. J.* **2012**, *18*, 8092–8099.

[27] Y. Li, J. Ding, M. Day, Y. Tao, J. Lu, M. D′iorio, *Chem. Mater.* **2004**, *16*, 2165–2173.

[28] D. Liu, H. C. Ren, J. Y. Li, Q. Tao, Z. X. Gao, *Chem. Phys. Lett.* **2009**, *482*, 72–76.

[29] P. Sonar, M. S. Son, Y. H. Cheng, J. T. Henssler, A. Sellinger, *Org. Lett.* **2010**, *12*, 3292–3295.

[30] CCDC-927618 (for **5**) and -927619 (for **8**) contains the supplementary crystallographic data for this paper. These data can be obtained free of charge from The Cambridge Crystallographic Data Centre via www.ccdc.cam.ac.uk/data_request/cif.

[31] M. C. Burla, M. Camalli, B. Corrozzini, G. L. Cascarano, C. Giacovazzo, G. Olidori, R. Spagna, *J. Appl. Crystallogr.* **2013**, *36*, 1103.

[32] G. M. Sheldrick, *Acta Crystallogr.* **2008**, *A46*, 112–122.

Received: April 4, 2013
Published Online: ■

Pyrene-Based Helicenes

A convenient route to a new class of pyrene-based [4]helicenes is presented along with their optoelectronic properties. The introduction of two methyl groups in the fjord region of the [4]helicene gives a more distorted structure and leads to a remarkable redshift of the absorption band.

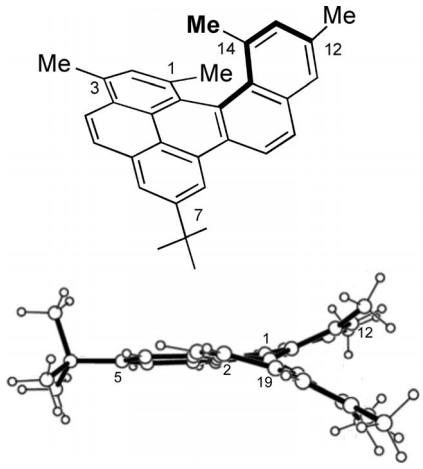

Keywords: Fused-ring systems / Wittig reactions / Cyclization / Helical structures / Optoelectronic properties

